

ZnO nanorod surface modification with PDDA/PSS Bi-layer assembly for performance improvement of ZnO piezoelectric energy harvesting devices

Jalali, N; Briscoe, J; Tan, YZ; Woolliams, P; Stewart, M; Weaver, PM; Cain, MG; Dunn, S

© 2014, Springer Science+Business Media

This is a pre-copyedited, author-produced version of an article accepted for publication in Journal of Sol-Gel Science and Technology following peer review. The version of record is available <https://link.springer.com/article/10.1007%2Fs10971-014-3512-4>

For additional information about this publication click this link.

<http://qmro.qmul.ac.uk/xmlui/handle/123456789/10893>

Information about this research object was correct at the time of download; we occasionally make corrections to records, please therefore check the published record when citing. For more information contact scholarlycommunications@qmul.ac.uk

ZnO Nanorod Surface Modification With PDDA/PSS Bi-Layer Assembly For Performance Improvement Of ZnO Piezoelectric Energy Harvesting Devices

Nimra Jalali¹, Joe Briscoe¹, Yan Zhi Tan², Peter Woolliams³, Mark Stewart³, Paul M. Weaver³,
Markys G. Cain³ and Steve Dunn,^{*1}

¹Queen Mary University of London, UK, ²Nan Yang Polytechnic, Singapore, ³National Physical Laboratory, UK

1. Abstract

ZnO nanostructure based energy harvesting devices (ZnO nanogenerator) were fabricated using ZnO nanorods with the surface modified using a polyelectrolyte assembly comprising bi-layers of PDADMAC (Polydiallyldimethylammonium chloride) and PSS (Polystyrene sulfonate). The peak open-circuit voltage device characteristics and power delivered across a load increased in relation to the number of bi-layers in the polyelectrolyte deposition. At the highest loading of polyelectrolyte the energy harvesters generated a peak power density of $426 \mu\text{W cm}^{-2}$ and 1 V peak open-circuit voltage at a peak tip acceleration of 50g. This compares to $35 \mu\text{W cm}^{-2}$ without polyelectrolyte. We relate this significant enhancement in device performance to the screening of mobile carriers due to an interaction of the polar polyelectrolyte materials with the surface of the ZnO nanostructures. It is proposed that the adsorption of the polyelectrolyte on the ZnO interacts with the surface defects and reduces the rate of screening and trapping of carriers leading to increased performance.

2. Introduction

Increasing interest in smart technologies directs our attention toward functional materials such as ZnO as a possible low cost solution to energy needs. ZnO is gaining significant interest due to the ability to be produced in a highly oriented manner at a low temperature, on flexible substrates, with associated nanostructured growth and texture [1]. This enables ZnO to be embedded into compact energy harvesting devices often termed nanogenerators. The efficiency of such devices requires consideration and in-depth analysis of various factors such as free charge carrier screening [2,3], series resistance and load capacitance. Evidence shows that in nanostructured ZnO a considerable screening of the ZnO polarisation comes from the surface-state charges and surface defects. The surface of ZnO is reported to be comprised of native defects and environmentally adsorbed impurities [3–7] which increase the carrier density in ZnO. These defects influence the internal rate of screening of strain-induced polarisation charges [2,3,8] and change the properties of the material.

Layer-by-layer deposition of polyelectrolytes is a widely used surface modification technique which provides benefits of controlled thickness at nanometer scale. Using this technique, two oppositely charged polyelectrolytes are alternately deposited on a solid surface and the adhesion of these layers is driven by the electrostatic interaction. Multilayers of polyelectrolytes can be formed by several repeated deposition steps of the charged polymers [9]. The adsorption [10] of polyelectrolytes on oppositely charged surfaces depends on variable factors such as temperature conditions, ionic strength and pH of solvent, temperature and molar concentration of the polyelectrolyte solution [11]. Similarly, the adhesion of multilayers of oppositely charged polyelectrolytes was reported to be dependent on the salt concentration and charge concentration of the polyelectrolyte [12].

Here we report the suppression of surface states using a layer-by-layer coating technique. Bi-layers of PDADMAC and PSS were used as surface modifiers in a Poly(3,4-ethylenedioxythiophene) Polystyrene sulfonate (PEDOT:PSS)/ZnO p-n junction-based energy harvesting device [2,3,8]. The resulting improvement in the nanogenerator performance is analysed and discussed. We show that the initial deposition of the polyelectrolyte was not sufficient to completely modify the surface of the ZnO. An optimum number of layers is established which is defined as the number of layers to modify surface behaviour but not produce excess series resistance for the extraction of current. This gives a peak open-circuit voltage output of 1.0 ± 0 V and peak power density of $426\pm 42 \mu\text{W cm}^{-2}$ across optimum load resistance of $11\pm 1 \text{ k}\Omega$.

3. Methods

ZnO nanorods were synthesized on $2\times 1 \text{ cm}^2$ ZnO seeded PET/ITO (polyethylene/indium tin oxide) substrates (Aldrich, surface resistivity $60 \Omega/\text{square}$). A precursor solution of 25 mM equimolar concentration of $\text{Zn}(\text{NO}_3)_2$ (Alfa Aesar, 99%) and HMT (Alfa Aesar, 99+%) in DI water was used. ZnO nanorod syntheses were performed for 2.5 hours at 90°C and repeated 6 times to obtain $2 \mu\text{m}$ long and 60 nm wide nanorods. The ZnO nanorod substrate was first dip-coated into 10 wt%, 3.58 pH, aqueous solution of PDADMAC and rinsed with DI water. Subsequently, the substrate was dip-coated into 10 wt% aqueous solution of PSS to form one bi-layer of polyelectrolytes. In 2 bi-layer and 4 bi-layer devices, this step was performed two and four times respectively; the devices fabricated with these nanorods were named as 2 bi-layer and 4 bi-layer devices. For the non-passivated device, this polyelectrolyte deposition step was omitted. Two layers of PEDOT:PSS were spin-coated at 2000 rpm on top of the coated and non-coated nanorods and each layer was dried at 100°C . A gold electrode was sputtered on top of PEDOT:PSS and wires were connected to the gold electrode and ITO. The $2\times 1 \text{ cm}^2$ device was mounted on a $500 \mu\text{m}$ thick plastic substrate. The devices were bent to produce a deflection of $\approx 6 \text{ mm}$ using a cam connected to rotating motor shaft and released with a resulting peak acceleration of the tip of 50 g [3,13].

The generated open-circuit voltage was measured using National Instruments NI PXI-4461 (24-bit ADC) on the NI PXIe-1062Q chassis. The resistive load matching was performed using NI PXI-4461 connected with Meatest M602 programmable decade box. Short-circuit current was measured using NI PXI-4461 connected with Low-Noise Current Preamplifier SR570. The calculations of energy density and charge displaced were performed using the mathematical techniques reported in previous work [8]. For each device, the output voltage cycle across the matched load resistance was recorded. The power delivered in the voltage cycle was integrated over the cycle duration to obtain the energy delivered to the load, given by [8]:

$$E = \int_{t_1}^{t_2} \frac{V(t)^2}{R} dt$$

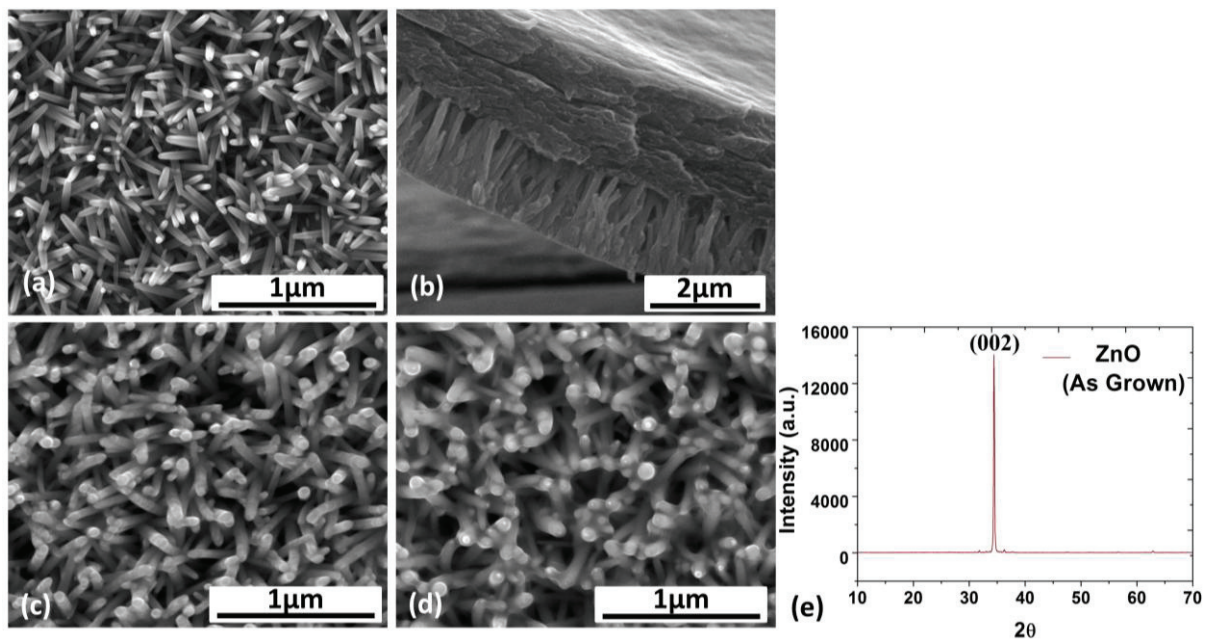
Similarly, the charge transferred to the load was obtained when the current delivered by the voltage cycle was integrated over the cycle duration, given by [8]:

$$Q = \int_{t_1}^{t_2} I(t) dt$$

1 The impedance analysis was performed using Agilent 4294A Precision Impedance Analyzer at a
2 frequency range of 40 Hz to 110 MHz. The X-ray diffraction was performed using X'Pert PRO MPD
3 θ -2 θ System in θ -2 θ Bragg-Brentano configuration with a diffracted beam monochromator.

4. Results and Discussion

4 Examples of as-grown nanorods top view (Figure 1(a)) and cross-section (Figure 1(b)) clearly show
5 that there is a well-oriented array of ZnO nanostructures. A prominent (002) peak was observed at
6 34.4° from the XRD analysis (Figure 1(e)) which confirmed the growth along the [0001] hexagonally
7 indexed c-direction. The PEDOT:PSS (p-type contact) was deposited on top of the nanorods to a
8 depth of ca. 250 nm. Figure 1(c) and (d) show the 2 and 4 bi-layer layer-by-layer self-assembly of
9 PDADMAC and PSS on ZnO nanorods. Figure 2 demonstrates the device measurements of open-
10 circuit voltage and short-circuit current density output from which peak values were obtained. To
11 fully determine the device performance parameters resistive load matching was performed obtaining
12 peak maximum power density across an optimum load (Figure 2(c)). The performance
13 characterisation clearly demonstrates the increase in the peak open-circuit voltage and peak power
14 density from the polyelectrolyte-coated ZnO nanorod devices (Table 1, Figure 2). The peak open-
15 circuit voltage increased 4 and 8 times when 2 and 4 bi-layers of PDDA and PSS coated ZnO surface.
16 The resistive load matching of 2 and 4 bi-layer devices demonstrated peak power densities of
17 $185 \mu\text{W cm}^{-2}$ and $426 \mu\text{W cm}^{-2}$ were obtained across an optimum load of $7.5 \text{ k}\Omega$ and $11 \text{ k}\Omega$. When
18 compared to a non-coated ZnO device, the peak power density of the 4 bi-layer polyelectrolyte device
19 was one order of magnitude higher.



20
21
22
23
24
25
26
27
28
29
30
31
32
33
34
35
36
37
38
39
40
41
42
43
44
45
46
47
48
49
50
51
52
53
54
55
56
57
58
59
60
61
62
63
64
65
Figure 1. SEM images: (a) as grown ZnO nanorod arrays (b) PEDOT:PSS deposited on top of nanorod arrays (c)
2 Bi layer self-assembly of PDADMAC and PSS (d) 4 Bi layer self-assembly of PDADMAC and PSS (e) XRD
spectrum of as-grown ZnO nanorod arrays.

Table 1. Performance parameters of the nanogenerators with and without coated nanorods.

Device	Open Circuit Voltage	Short Circuit Current	Optimum Load Resistance	Peak Power Density	Peak Power/cm ³	Energy Density	Charge Displaced	Time Constant
	mV	mA/cm ²	kΩ	μW/cm ²	W/cm ³	nJ/cm ²	nC/cm ²	ms
ZnO (As Grown)	121	1.02	1	35	0.14	5.5	129	0.016
2 Bi layers	480	1.30	7.5	185	0.75	65	344	0.33
4 Bi Layers	1000	1.47	11	426	1.70	144	398	1.33

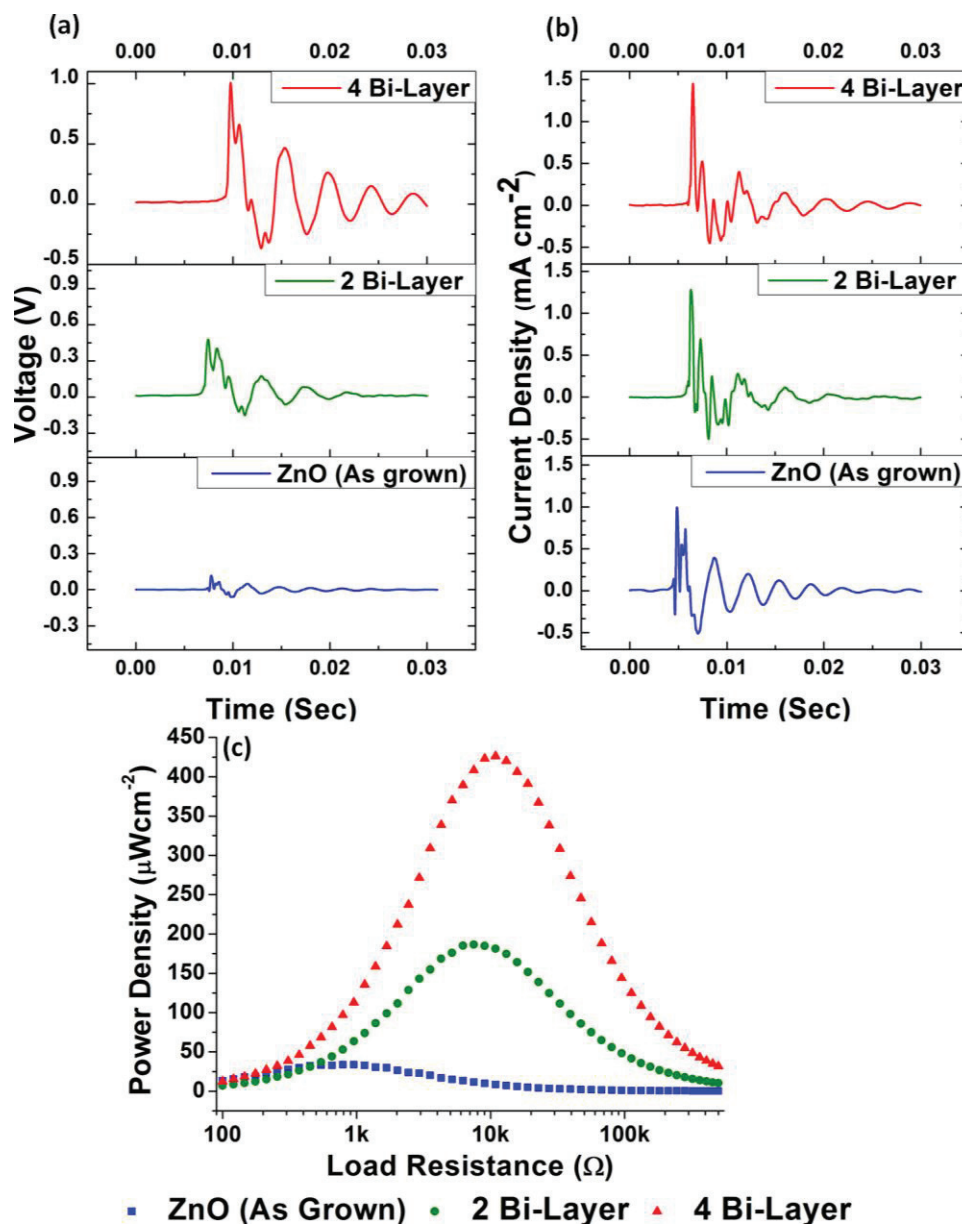


Figure 2. Measured performance of the nanogenerators with non-coated and coated nanorods: (a) open-circuit voltage (b) short-circuit current (c) resistive load matching.

1 We have focused on passivation of the ZnO surface using polyelectrolytes, which are charged
2 polymer chains capable of adsorption onto oppositely charged surfaces [14,15]. It has been found that
3 ZnO has a negative surface charge in aqueous solutions [16]. Therefore, as PDADMAC is a cationic
4 solution, a layer will adsorb on the ZnO due to electrostatic attraction and cause a charge reversal of
5 the ZnO surface [16]. Subsequent deposition of anionic PSS produces another charge reversal to
6 leave the surface negative [17]. We are therefore able to produce a layer-by-layer assembly of
7 polyelectrolyte which can be further increased to form a multilayer assembly [17].
8

9
10 The first deposition of a bi-layer will adsorb at high surface free energy locations and may not give
11 complete coverage. During this first deposition cycle adding the anionic second polyelectrolyte
12 component of the bi-layer will not add to the coverage of the ZnO. When the number of bi-layers is
13 increased, layers of polyelectrolytes will increase the coverage of the ZnO surface increasing the
14 packing density of the polyelectrolytes as they adhere strongly to the ZnO surface [18] [19]. As the
15 surface is more thoroughly covered in bi-layers, loosely bound polymer is removed through
16 equilibrium processes to leave only tightly bound material on the ZnO surface [14]. The near
17 conformally covered polyelectrolyte layers act to isolate the functional nanorod from its environment,
18 thereby reducing the concentration of mobile charge carriers present on the surfaces of bare ZnO
19 nanorods. The ZnO surface-coated bi-layer structure exhibits an increase in power output such that at
20 4 bi-layers the device generated a peak open-circuit voltage output of 1 V and with a peak power
21 density of $426 \mu\text{W cm}^{-2}$. This effect of performance improvement is linked with the decrease in the
22 rate of internal screening of polarisation charges due to a decrease in free charge carrier density in
23 surface-coated ZnO. We are therefore able to show that surface passivation through the generation of
24 a polyelectrolyte bi-layer can significantly enhance the power output from a nanostructured ZnO
25 energy harvesting device. The dynamic response of the measurement equipment (24bit ADC) was at
26 least one order of magnitude faster than the mechanical (cam) cyclic excitation providing sufficient
27 resolution for reliable measurement of the voltage, current and peak power. Furthermore, for this
28 performance comparison between uncoated and coated systems, an identical measurement apparatus
29 was used throughout producing comparable datasets. This often disregarded issue pertaining to peak
30 measurement data is important and unless carefully assessed can give rise to misleading or inaccurate
31 comparisons.
32

33
34 An Agilent 4294A Impedance Analyser was used to characterise the devices for their impedance
35 response to input frequency sweep ranged between 40 Hz - 110 MHz. The results were presented as
36 Nyquist plots (Figure 3 (a-c)); the time constant (τ_{RC}) for each device was calculated from the critical
37 frequency ($\tau_{RC} = \frac{1}{f_c}$) of the semi-circle with largest diameter (see Ref [3] for details). A correlation
38 between devices' time constant (τ_{RC}) and their voltage output was observed which was in agreement
39 to our previous results reported in reference [3]. For non-coated ZnO device, the calculated time
40 constant was 0.016 ms whereas, the same measurement for the 4-bilayer ZnO surface modified device
41 was 2 orders of magnitude higher ($\tau_{RC} = 1.33$ ms, Table 1). This result was reported to be caused by
42 the suppression of surface-states in coated-ZnO, which reduced the free carrier density and therefore
43 decreased the rate of internal polarisation field screening in ZnO nanorods [3]. Hence, the duration of
44 the polarisation field in ZnO, represented by the time constant (τ_{RC}), increased which increased the
45 potential difference across the ZnO. Consequently, the measured peak open-circuit voltage of coated
46 devices was higher than the non-coated device. Therefore this correlation between device time
47 constant (τ_{RC}) and peak open-circuit voltage explains the phenomenon of internal polarisation field
48 screening caused by ZnO surface-state injected free carriers.
49
50
51
52
53
54
55
56
57
58
59
60
61
62
63
64
65

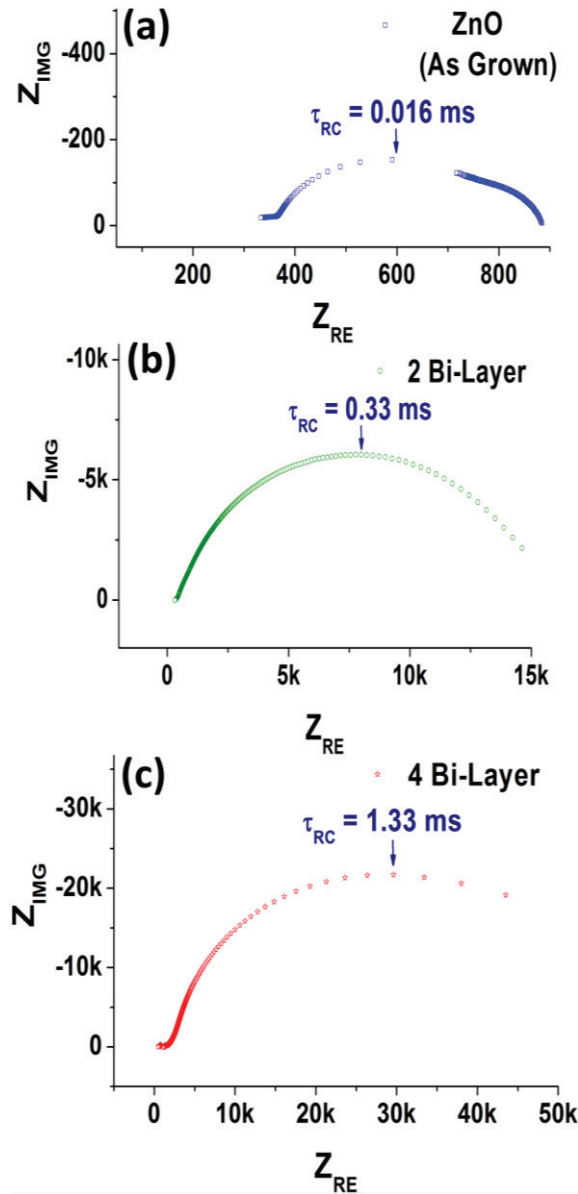


Figure 3. Nyquist plots extracted from impedance spectroscopy measurement of: (a) uncoated, (b) 2 Bi-layer and (c) 4 Bi-layer devices with time constants of 0.016 ms, 0.33 ms and 1.33 ms as indicated on the plots.

5. Conclusion

We show that increasing the surface coverage of a polyelectrolyte bi-layer structure can enhance the energy harvesting potential of a ZnO nanostructured device. The peak open-circuit voltage increased 8 times when 4 bi-layers of PDDA and PSS were coated on ZnO surface, compared to the uncoated device. Similarly, the peak power density of 4 bi-layer device was obtained as $426 \mu\text{W cm}^{-2}$ which was an order of magnitude higher than the non-coated ZnO device. The process by which device performance is improved is associated with the screening of mobile carriers in the ZnO and the influence of the polyelectrolyte on charge-balancing charged defects at the ZnO surface. The device performance parameters were further analysed using impedance analysis, which demonstrates a correlation between device peak open-circuit voltage output and time constant (τ_{RC}) of the equivalent RC circuit.

6. Acknowledgement

This work was supported by the European Metrology Research Programme (EMRP), jointly funded by the EMRP participating countries within EURAMET and the European Union. The work is also supported by the UK's National Measurement Office, BIS, UK Government.

References

- [1] Greene L E, Yuhas B D, Law M, Zitoun D and Yang P 2006 Solution-grown zinc oxide nanowires. *Inorg. Chem.* **45** 7535–43
- [2] Briscoe J, Stewart M, Vopson M, Cain M, Weaver P M and Dunn S 2012 Nanostructured p-n Junctions for Kinetic-to-Electrical Energy Conversion *Adv. Energy Mater.* **2** 1261–8
- [3] Jalali N, Woolliams P, Stewart M, Weaver P M, Cain M G, Dunn S and Briscoe J 2014 Improved performance of p–n junction-based ZnO nanogenerators through CuSCN-passivation of ZnO nanorods *J. Mater. Chem. A* **2** 10945
- [4] Hu Y, Lin L, Zhang Y and Wang Z L 2012 Replacing a battery by a nanogenerator with 20 V output. *Adv. Mater.* **24** 110–4
- [5] Janotti A and Van de Walle C G 2009 Fundamentals of zinc oxide as a semiconductor *Reports Prog. Phys.* **72** 126501
- [6] Hatch S M, Briscoe J, Sapelkin A, Gillin W P, Gilchrist J B, Ryan M P, Heutz S and Dunn S 2013 Influence of anneal atmosphere on ZnO-nanorod photoluminescent and morphological properties with self-powered photodetector performance *J. Appl. Phys.* **113** 204501
- [7] Pham T T, Lee K Y, Lee J-H, Kim K-H, Shin K-S, Gupta M K, Kumar B and Kim S-W 2013 Reliable operation of a nanogenerator under ultraviolet light via engineering piezoelectric potential *Energy Environ. Sci.* **6** 841
- [8] Briscoe J, Jalali N, Woolliams P, Stewart M, Weaver P M, Cain M and Dunn S 2013 Measurement techniques for piezoelectric nanogenerators *Energy Environ. Sci.* **6** 3035
- [9] Wang Y, Wang S, Xiao M, Han D, Hickner M A and Meng Y 2013 Layer-by-layer self-assembly of PDDA/PSS-SPFEK composite membrane with low vanadium permeability for vanadium redox flow battery *RSC Adv.* **3** 15467
- [10] Feuz L, Höök F and Reimhult E 2012 Design of Intelligent Surface Modifications and Optimal Liquid Handling for Nanoscale Bioanalytical Sensors *Intelligent Surfaces in Biotechnology* (John Wiley & Sons, Inc.) pp 71–122
- [11] Mehrotra S, Hunley S C, Pawelec K M, Zhang L, Lee I, Baek S and Chan C 2010 Cell adhesive behavior on thin polyelectrolyte multilayers: cells attempt to achieve homeostasis of its adhesion energy. *Langmuir* **26** 12794–802

- 1
2
3
4
5
6
7
8
9
10
11
12
13
14
15
16
17
18
19
20
21
22
23
24
25
26
27
28
29
30
31
32
33
34
35
36
37
38
39
40
41
42
43
44
45
46
47
48
49
50
51
52
53
54
55
56
57
58
59
60
61
62
63
64
65
- [12] Van de Steeg H G M, Cohen Stuart M A, De Keizer A and Bijsterbosch B H 1992 Polyelectrolyte adsorption: a subtle balance of forces *Langmuir* **8** 2538–46
- [13] Briscoe J, Jalali N, Loh L, Shoaee S, Wooliams P, Stewart M, Cain M, Weaver P M, Durrant J R and Dunn S 2013 ZnO Nanostructured Diodes - Enhancing Energy Generation through Scavenging Vibration *MRS Proc.* **1556** mrss13–1556–w04–01
- [14] Knoll W and Advincula R C 2013 *Functional Polymer Films* (John Wiley & Sons)
- [15] Andelman D and Joanny J-F 2000 Polyelectrolyte adsorption *Comptes Rendus l'Académie des Sci. - Ser. IV - Phys.* **1** 1153–62
- [16] Lao C S, Park M-C, Kuang Q, Deng Y, Sood A K, Polla D L and Wang Z L 2007 Giant enhancement in UV response of ZnO nanobelts by polymer surface-functionalization. *J. Am. Chem. Soc.* **129** 12096–7
- [17] Lua Y-Y, Yang L, Pew C A, Zhang F, Fillmore W J J, Bronson R T, Sathyapalan A, Savage P B, Whittaker J D, Davis R C and Linford M R 2005 Polyelectrolytes as new matrices for secondary ion mass spectrometry. *J. Am. Soc. Mass Spectrom.* **16** 1575–82
- [18] Dodoo S, Balzer B N, Hugel T, Laschewsky A and Klitzing R von 2013 Effect of Ionic Strength and Layer Number on Swelling of Polyelectrolyte Multilayers in Water Vapour *Soft Mater.* **11** 157–64
- [19] Shin Y W, Roberts J E and Santore M 2001 The Influence of Charge Variation on the Adsorbed Configuration of a Model Cationic Oligomer onto Colloidal Silica *J. Colloid Interface Sci.* **244** 190–9